Observational constraints on the product of dark energy chemical potential and number density in out-of-equilibrium models

J. M. Costa Netto, 1, * Javier E. Gonzalez, 2, † and H. H. B. Silva 1, ‡

Núcleo de Formação Docente, Centro Acadêmico do Agreste,
 Universidade Federal de Pernambuco, Caruaru, Pernambuco, 55014-900, Brazil
 Departamento de Física, Universidade Federal de Sergipe, São Cristóvão, Sergipe, 49107-230, Brazil

In this work, we impose observational limits on the product of dark energy chemical potential, μ , and number density, n, at the present time in out-of-equilibrium models, considering that particles can be created or destroyed in the fluid at a rate $\Gamma = 3\alpha H(a)$, where α is a constant and $H(a) \equiv \dot{a}/a$ is the Hubble parameter. We combine the bounds derived from the positivity of entropy and the second law of thermodynamics with observational constraints on the Chevallier-Polarski-Linder (CPL) and Barboza-Alcaniz (BA) parameterizations of the equation of state (EoS) of the component. We use Type Ia supernovae (SN Ia) data from Pantheon+; baryon acoustic oscillation (BAO) data from DESI DR2; and cosmic microwave background (CMB) measurements from Planck. For $\alpha>0$ (particle creation), the thermodynamic restrictions yield only upper limits for the $\mu_0 n_0$ product, while in the case of $\alpha<0$ (particle destruction) they establish both upper and lower limits, allowing for a range of values to be obtained. In both scenarios, however, we find that the chemical potential of dark energy must be negative, $\mu<0$, which indicates a preference for the phantom regime. In particular, when $\alpha<0$, it is noted that the thermodynamic bounds are simultaneously compatible only for very small absolute values of α , with $\alpha=-0.0002$ being the limiting case and resulting in $\mu_0 n_0 (\alpha=-0.0002) = -2.2^{+1.0}_{-0.002} \ GeV/m^3$.

I. INTRODUCTION

Recent results obtained by the Dark Energy Spectroscopic Instrument (DESI) [1, 2] indicate, when combining its baryon acoustic oscillations (BAO) data with Type Ia supernovae (SN Ia) data [3-6] and cosmic microwave background (CMB) measurements [7, 8] from other collaborations, a preference toward dynamic dark energy models, more specifically models in which the equation of state (EoS) parameter of the component is a function of the scale factor a, w = w(a). There is also a preference for a transition between a phantom regime and quintessence scenarios, where w(a) < -1 and $|w(a)| \leq 1$, respectively. Although these conclusions are new and subject of much debate given their impact, the study of dark energy and, in particular, dynamical models, hence, becomes a topic of great relevance in the world of cosmology.

Dark energy can be studied, essentially, from two perspectives: one in which it is modeled by a relativistic fluid and the entire basis of thermodynamics is applied [9–14]; another in which it is associated with a scalar potential and field theory is used [15–18]. Although the two approaches are not incompatible, in this work we adopt the thermodynamic one. For models in which the barotropic EoS parameter

$$w(a) \equiv \frac{p_x}{\rho_x} = w_0 + w_a f(a), \tag{1}$$

where p_x and ρ_x are, respectively, the pressure and the dark energy density, w_0 and w_a are constants, and f(a) is a scale factor function (or, equivalently, time dependent), the fluid departs from the adiabatic regime and effectively behaves as if it possessed a bulk viscous pressure, generating entropy as an a posteriori effect [12, 13]. Independently of whether dark energy is in or out of equilibrium, the chemical potential, μ , is responsible for determining the range of possible values of w(a) [10, 11, 13]: if $\mu < 0$, the component will be in the phantom regime; if $\mu = 0$, the cosmological constant is recovered; if $\mu > 0$, neither of these two cases is reached.

In cosmology, it is well known that bulk viscosity is closely related to particle creation or destruction processes. Indeed, it is possible to phenomenologically describe bulk viscous pressures through particle sources or sinks [19–23]. Bearing in mind that dark energy begins to mimic a bulk viscous pressure as a consequence of a variable EoS, it is reasonable to assume the possibility of particles being created or destroyed in the fluid. In [24] we consider exactly that by proposing

$$N^{\mu}_{\;\;;\mu} = n\Gamma, \qquad (2)$$

where N^{μ} is the particle current vector, n is the number density, and Γ is the rate of particle creation $(\Gamma > 0)$ or destruction $(\Gamma < 0)$. This, of course,

^{*} jose.medeiroscn@gmail.com

[†] javiergonzalezs@academico.ufs.br

 $^{^{\}ddagger}$ heydson.henrique@ufpe.br

adds a new term to the entropy source and, therefore, affects not only the evolution of n, but also the entropy density s. However, since the energy-momentum tensor $T^{\mu\nu}$ is unaffected, the continuity equation and thus the evolution of the dark energy density remains the same — as does the temperature evolution law, since it depends only on the EoS.

Although we perform an initial generalization of the out-of-equilibrium thermodynamic models of dark energy, we did not specify a functional form for the Γ -term in [24]. Based on [23], in this present work we adopt the expression

$$\Gamma = 3\alpha H(a),\tag{3}$$

where α is assumed to be constant and can be positive (particle creation) or negative (particle destruction), and $H(a) \equiv \dot{a}/a$ is the Hubble parameter. Our objective is to impose observational constraints on $\mu_0 n_0$, the present time value of the product of the chemical potential and the number density, using the bounds derived from the positivity of entropy and the second law of thermodynamics.

This work is organized as follows: in Section II, we review the model proposed in [24]. Starting from the fundamental equations that describe the fluid, we arrive at expressions for the entropy and the entropy source that allow us to obtain the thermodynamic bounds mentioned above. We combine these limits with observational constraints on the Chevallier-Polarski-Linder (CPL) [25, 26] and Barboza-Alcaniz (BA) [27] parameterizations of the barotropic EoS parameter of dark energy. To this end, we rely on SN Ia data from Phanteon+ [3, 4]; BAO data from DESI DR2 [2]; and CMB measurements from Planck [7, 8]. These datasets and its respective statistical treatment are contained in Section III (and in Appendix A). The limits imposed on the product of chemical potential and particle density are found in Section IV (and in Appendix A), along with a detailed discussion of their implications. In Section V, we present the conclusions of the research.

Throughout this work, we use the subscript 0 to indicate quantities measured at the present time, $t = t_0$, and, unless otherwise stated, we adopt units in which $8\pi G = c = 1$ and $a(t_0) = a_0 = 1$. Our metric signature is (+, -, -, -).

II. OUT-OF-EQUILIBRIUM DARK ENERGY THERMODYNAMICS

When working with relativistic hydrodynamics, the basic tensors of the dark energy fluid in a flat Friedmann-Lemaître-Robertson-Walker (FLRW) universe are [28, 29]:

$$T^{\mu\nu} = \rho_x U^{\mu} U^{\nu} - p_x h^{\mu\nu}, \tag{4}$$

$$N^{\mu} = nU^{\mu},\tag{5}$$

$$S^{\mu} = sU^{\mu} = n\sigma U^{\mu},\tag{6}$$

where U^{μ} is the 4-velocity, $h^{\mu\nu} \equiv g^{\mu\nu} - U^{\mu}U^{\nu}$ is the projector onto the local rest space of the 4-velocity, S^{μ} is the entropy current vector, and σ is the specific entropy.

If the fluid is outside the adiabatic limit, we introduce the variations $\Delta T^{\mu\nu}$ and ΔN^{μ} in Eq. (4) and Eq. (5), respectively [30]:

$$T^{\mu\nu} = \rho_x U^{\mu} U^{\nu} - p_x h^{\mu\nu} + \Delta T^{\mu\nu}, \tag{7}$$

$$N^{\mu} = nU^{\mu} + \Delta N^{\mu}. \tag{8}$$

The Eckart [31] and Landau-Lifshitz [32] approaches are the most common in cosmology when it comes to non-equilibrium thermodynamics. Although the former defines U^{μ} as the 4-velocity of particle transport and the latter defines it as the 4-velocity of energy transport, both formalisms consider that the out-of-equilibrium terms present in Eqs. (7, 8) are small enough to consider only first-order deviations. Assuming that scalar processes are the only dissipative effects occurring in dark energy, it can be shown that [30]

$$U_{\mu}\Delta T^{\mu\nu}_{:\nu} = (\Pi + p_c)\Theta, \tag{9}$$

$$\Delta N^{\mu}_{\ :\mu} = 0,\tag{10}$$

where Π is the bulk viscous pressure, p_c is the creation pressure, and $\Theta \equiv 3H(a)$ is the expansion rate of the fluid. The creation pressure p_c is associated with the adiabatic matter creation processes [33–35]. Considering that, in cosmology, we can relate the creation or destruction of particles to the bulk viscosity [19–23], the p_c -term becomes, to some extent, redundant. Thus, without loss of generality,

$$U_{\mu}\Delta T^{\mu\nu}_{\ \ \nu} = \Pi\Theta. \tag{11}$$

Using Eq. (1), the null divergence of $T^{\mu\nu}$ projected in the 4-velocity direction leads to the continuity equation:

$$U_{\mu}T^{\mu\nu}_{:\nu} = \dot{\rho}_x + 3H(a)(\rho_x + p_{eq}) = -3H(a)\Pi, (12)$$

where $p_{eq} \equiv w_0 \rho_x$ is the equilibrium pressure and $\Pi = w_a f(a) \rho_x$ is the bulk viscous pressure mimicked by the dark energy fluid [12, 13]. According to Eq. (2), the particle balance equation becomes [24]:

$$N^{\mu}_{...} = \dot{n} + 3H(a)n = n\Gamma.$$
 (13)

Consequently, the new entropy source of the component is [24]:

$$S^{\mu}_{\ \mu} = n\dot{\sigma} + n\sigma\Gamma. \tag{14}$$

Setting $S^{\mu}_{\;\;;\mu} \geq 0$ in Eq. (14), we get $\Gamma \geq -\dot{\sigma}/\sigma$. If $\dot{\sigma}=0$, as in the cosmological fluid [33–35], $\Gamma \geq 0$ and particles can only be created — in this case, it is common to use p_c instead of Π in Eq. (11). In the non-adiabatic scenario, we also get particle creation if $\dot{\sigma} < 0$. Particle destruction, $\Gamma < 0$, is possible as long as $\dot{\sigma} > 0$. Since there is no special reason to take $\dot{\sigma} = 0$ for dark energy, particles can be not only created but also destroyed, and this does not violate the second law of thermodynamics or any other. In fact, considering that in models with $\Gamma = 0$ the source of entropy is $S^{\mu}_{\;\;;\mu} = n\dot{\sigma}$, assuming $\dot{\sigma} = 0$ is a direct contradiction to the conclusion that the fluid leaves the adiabatic limit and begins to suffer from bulk viscosity when its barotropic EoS parameter varies with time [12, 13]. Therefore, a priori, both processes of particle creation or destruction are possible.

Another relevant aspect concerns the effect of Γ on the Hubble parameter and the possibility of constraining it observationally. The processes of matter creation in cosmology have been the subject of long-standing debate. In the case where the cosmological fluid satisfies $\dot{\sigma}=0$, only particle creation processes are allowed [33–35]. Under this condition, it is possible to derive a relation between the bulk viscous pressure and Γ such that Γ enters the continuity equation and, consequently, contributes explicitly to the Hubble parameter:

$$\Gamma = -\frac{3H(a)\Pi}{\rho_x + p_{eq}}. (15)$$

We emphasize, however, that Eq. (15) is only valid in the context of the adiabatic creation of matter discussed in [33–35]. In the more general scenario we are interested in, $\dot{\sigma} \neq 0$, there is no well-defined expression in theory for Γ or relationships between Γ and Π . In such cases, one must rely on phenomenological prescriptions. For example, in [19] it is used

$$\Gamma = -\frac{1}{\beta} 3H(a)\Pi, \tag{16}$$

where β is a constant. Although the above expression is an ansatz, it takes into account, as pointed by the authors, particle creation processes in which the generated entities are in thermal equilibrium with the energy-material content already present in the cosmological fluid, so that these processes become the sole cause of entropy production in the cosmos. Therefore, β is defined as positive, so that Π is negative. In our work, we sought, based on [23], to adopt a more general functional form for Γ that would not depend on scenarios such as the one described in [33–35] or the one assumed in [19]. Thus, we use the expression given in Eq. (3),

$$\Gamma = 3\alpha H(a)$$
.

This relation does not link Π and Γ and, therefore, does not allow the rate of particle creation or destruction to affect the Hubble parameter. For this to be possible, it would be necessary to have a functional form for Γ that relates this term to the energy-momentum tensor of dark energy, i.e., a functional form that connects it to the bulk viscous pressure without considering adiabatic scenarios. However, this is not the objective of this work.

Applying the functional form for the Γ -term given in Eq. (3), the solutions to Eqs. (12, 13) are, respectively [12, 13, 24]:

$$\rho_x = \rho_{x,0} a^{-3(1+w_0)} \exp\left(-3w_a \int_1^a f(\tilde{a}) \frac{d\tilde{a}}{\tilde{a}}\right) \quad (17)$$

and

$$n = n_0 a^{-3(1-\alpha)}. (18)$$

In [24], we verified that the temperature evolution law presented in [12, 13] continues to hold. Then

$$\frac{\dot{T}}{T} = -3H(a) \left[\left(\frac{\partial p_0}{\partial \rho_x} \right)_n + \left(\frac{\partial \Pi}{\partial \rho_x} \right)_n \right]$$
(19)

and, therefore,

$$T = T_0 a^{-3w_0} \exp\left(-3w_a \int_1^a f(\tilde{a}) \frac{d\tilde{a}}{\tilde{a}}\right).$$
 (20)

Assuming that the relation $\mu/T = \mu_0/T_0$ [10, 11] remains valid in the non-equilibrium context, the

Euler relation for thermodynamics leads us to the specific entropy of the fluid [24]:

$$\sigma = \frac{\rho_{x,0}}{n_0 T_0} (1 + w_0 + w_a f(a)) \frac{1}{a^{3\alpha}} - \frac{\mu_0}{T_0}.$$
 (21)

Thus,

$$\dot{\sigma} = \frac{\rho_{x,0}}{n_0 T_0} \left[w_a a f'(a) - 3\alpha (1 + w_0 + w_a f(a)) \right] \frac{H(a)}{a^{3\alpha}}.$$
(22)

Note that $\dot{\sigma}$ can mathematically be either positive or negative, as we expected. The entropy density is:

$$s = \left[s_0 + \rho_{x,0}(w(a) - w_0) - \mu_0 n_0(a^{3\alpha} - 1)\right] \frac{1}{T_0 a^3}.$$
(23)

With these quantities determined, we can obtain the entropy and entropy source of dark energy in out-of-equilibrium models.

Since $S = (n\sigma)V$ is the total entropy, where $V = V_0 a^3$ is the comoving volume [28, 29], we get [24]:

$$S = \left[\rho_{x,0}(1 + w_0 + w_a f(a)) - \mu_0 n_0 a^{3\alpha}\right] \frac{V_0}{T_0}.$$
 (24)

Substituting Eqs. (18, 21, 22) into Eq. (14), the entropy source of the fluid is obtained:

$$S^{\mu}_{;\mu} = \left[w_a f'(a) \rho_{x,0} - 3\alpha \mu_0 n_0 a^{3\alpha - 1} \right] \frac{H(a)}{T_0 a^2}. \quad (25)$$

Before getting to the thermodynamic constraint equations for $\mu_0 n_0$, it is interesting to note that $S \geq 0$ leads us to $w(a)_{min} = -1 + (\mu_0 n_0/\rho_{x,0}) a^{3\alpha}$. As we can see, if $\mu < 0$, then $w(a)_{min} < -1$ and dark energy is in the phantom regime; if $\mu = 0$, then $w_{min} = -1$ and the cosmological constant scenario is recovered; if $\mu > 0$, then $w(a)_{min} > -1$.

Imposing the positivity of entropy on Eq. (24), we arrive at an upper limit for the product of the chemical potential and the particle density:

$$\mu_0 n_0 \le (1 + w_0 + w_a f(a)) \frac{\rho_{x,0}}{a^{3\alpha}}.$$
 (26)

From the second law of thermodynamics,

$$\alpha \mu_0 n_0 \le \frac{w_a f'(a)}{3a^{3\alpha - 1}} \rho_{x,0}.$$
 (27)

We have two possibilities depending on the sign of α : if it is positive, we will obtain another upper bound for $\mu_0 n_0$ different from the one derived from $S \geq 0$;

if it is negative, Eq. (25) will lead us to a lower limit for this product. In summary, we can write:

$$\mu_0 n_0 \begin{cases} \leq \frac{w_a f'(a)}{3\alpha a^{3\alpha - 1}} \rho_{x,0}, & \alpha > 0, \\ \geq \frac{w_a f'(a)}{3\alpha a^{3\alpha - 1}} \rho_{x,0}, & \alpha < 0. \end{cases}$$
(28)

As we can see, thermodynamics will not necessarily produce upper and lower bounds for the product $\mu_0 n_0$. This will depend on the sign of the constant α . In any case, Eqs. (26, 28) are sufficient to impose observational constraints and restrict the possible values for this quantity.

III. OBSERVATIONAL DATA AND STATISTICAL ANALYSES

As demonstrated in Section II, the product of the chemical potential and the number density of dark energy is constrained by thermodynamic considerations. The positivity of the entropy defines an upper bound (\hat{l}_{\sup}^{PE}) for $\mu_0 n_0$, while the second law of thermodynamics imposes an additional constraint: an upper bound $(l_{\text{inf}}^{\text{SL}})$ for positive values of α and a lower bound $(l_{\text{inf}}^{\text{SL}})$ for negative values of α . These thermodynamic limits depend on the redshift, the parameter α and cosmological parameters $(\Omega_m, H_0, w_0, w_a)$, which are statistically constrained by cosmological probes. In order to constrain $\mu_0 n_0$, we perform statistical analyses under the assumption of a spatially flat universe in which the dark energy component is modeled as a fluid characterized by the CPL and BA EoS. The following cosmological data are considered:

- SN Ia: The Pantheon+ compilation [3, 4] is employed, comprising 1701 light curves from 1550 spectroscopically confirmed supernovae, covering a redshift range from 0.01 up to 2.34. The apparent magnitude m serves as the relevant cosmological observable, being related to cosmic dynamics through the luminosity distance. The high quality and large volume of this dataset enable stringent constraints on the two-parameter dark energy models considered.
- BAO: Using approximately 14 million galaxy positions and redshifts, the DESI Collaboration has measured BAO signals with unprecedented precision [2]. Based on these data, five tracers¹ were employed to determine six

¹ Bright Galaxies (see [2] for details of the sample), Luminous

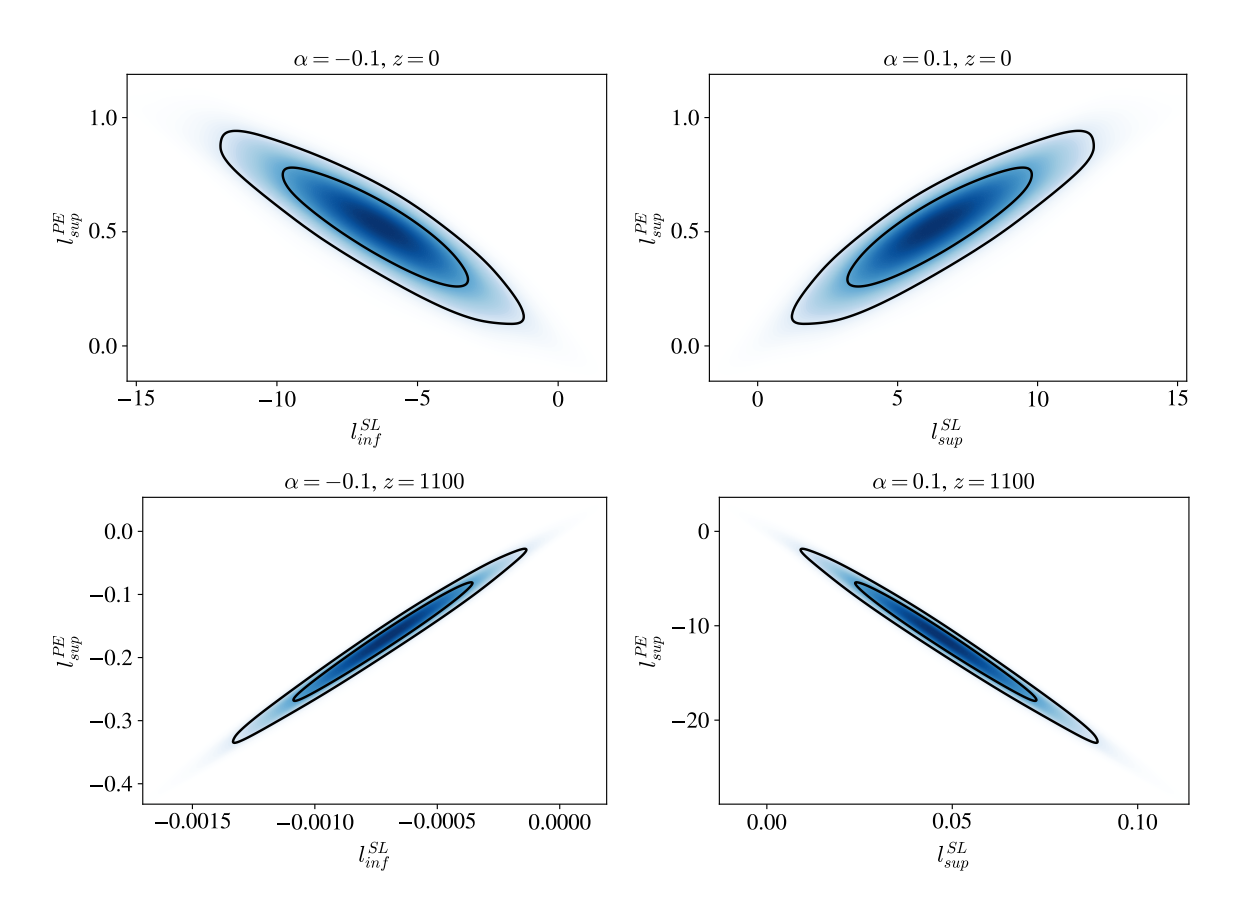


Figure 1. 1σ and 2σ confidence levels of the thermodynamic limits for two values of the parameter α and two redshifts in the CPL model.

independent measurements of the anisotropic BAO signal, yielding corresponding estimates of D_M/r_d and D_H/r_d over an effective redshift range of 0.510 to 2.330, as well as one isotropic measurement providing D_V/r_d at z=0.295.

• CMB: The temperature and polarization fluctuations in the CMB constitute one of the most powerful cosmological probes. Measurements from the Planck satellite [7, 8], in combination with other observational datasets, enable precise constraints on the energy density components of the universe and on the parameters of a two-parameter dark energy EoS. We employ the temperature (TT), temperature—polarization (TE), and polarization (EE) power spectra, adopting the Commander likelihood for the temperature spectrum and the SimAll likelihood for the polarization spectrum at low multipoles (l > 30), and the

Parameter Prior $\mathcal{U}[0.005, 0.1]$ $\omega_{b,0}$ $\mathcal{U}[0.001, 0.99]$ $\omega_{c,0}$ w_0 $\mathcal{U}[-3,1]$ U[-3, 2] w_a $\ln 10^{10} A_s$ U[1.61, 3.91] $\mathcal{U}[0.8, 1.2]$ n_s 100θ $\mathcal{U}[0.5, 10]$ $\mathcal{U}[0.01, 0.8]$ τ

Table I. Priors used for the MCMC analysis considering Pantheon+, DESI DR2, and Planck PR4 data. We assume uniform priors which are noted as $\mathcal{U}[\text{Min}; \text{Max}]$.

most recent CamSpec PR4 likelihood for the TT, TE, and EE spectra at high multipoles (l > 30) [36, 37]. In addition, we include the CMB lensing reconstruction power spectrum from the PR4 data [38].

To constrain the parameters of the aforementioned models, we use the *COBAYA* code [39] to perform Bayesian analyses through Markov chain

Red Galaxies, Emission Line Galaxies, Quasars, and the Ly- $\!\alpha$ Forest.

Monte Carlo (MCMC) from the Metropolis-Hasting sampler. We use the CLASS code [40] and a modification of it to compute the theoretical cosmological equations. Following the performed analysis in [2], the assumed priors are presented in Table I, where $\omega_{b,0}$ is the physical baryon density, $\omega_{c,0}$ is the physical dark matter density, w_0 and w_a are the usual parameters of the dark energy EoS, θ_s is the angular size of the sound horizon at recombination, A_s is the scalar amplitude, n_s is the spectral index and τ is the optical depth to reionization.

Table II summarizes the results of the statistical analyses of cosmological parameters related to the thermodynamic constraints for the CPL and BA parameterizations. This analysis was performed using the *GetDist* package [41].

Parameter	CPL	BA
$\Omega_{m,0}$		0.3104 ± 0.0058
H_0	$67.51^{+0.58}_{-0.61}$	67.59 ± 0.61
w_0	$\begin{array}{c} -0.850^{+0.053}_{-0.052} \\ -0.56^{+0.20}_{-0.21} \end{array}$	$-0.873^{+0.059}_{-0.046} \ -0.28^{+0.099}_{-0.10}$
w_a	$-0.56^{+0.20}_{-0.21}$	$-0.28^{+0.099}_{-0.10}$

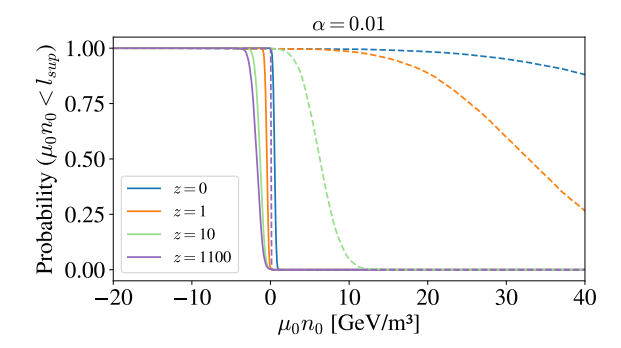
Table II. Marginalized results of the cosmological parameters that define the thermodynamic limits in Eqs. (26, 28).

Since the thermodynamic limits depend on the cosmological parameters, they can be regarded as random variables whose distributions, $P(l^{\text{SL}}, l^{\text{PE}})$, are derived from the posterior distributions of the cosmological parameters $\{\Omega_m, H_0, w_0, w_a\}$, and the α and the redshift values. In Figure 1, we present the bidimensional distributions of these limits for four combinations of values of α and z considering the CPL model. The results of the thermodynamic limits and the constraints on the product $\mu_0 n_0$ for the BA parameterization are presented in Appendix A.

IV. OBSERVATIONAL LIMITS ON THE $\mu_0 n_0$ PRODUCT

Since the product $\mu_0 n_0$ and the cosmological parameters are related through an inequality rather than a functional dependence, it is convenient to represent the cumulative probability that a given value of $\mu_0 n_0$ satisfies the corresponding upper or lower thermodynamic constraint. Mathematically, this can be written as

$$P(\mu_0 n_0 < l_{sup}) = \int_{\mu_0 n_0}^{\infty} P(l_{sup}) dl_{sup}$$
 (29)



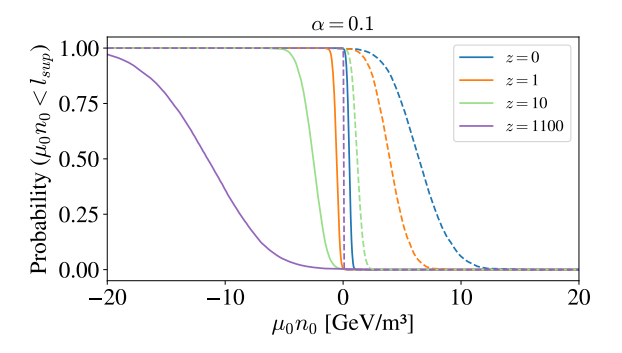


Figure 2. Probability that a given value of $\mu_0 n_0$ satisfies the thermodynamic conditions for positive values of α in the CPL model. The solid lines correspond to the bound of the positivity of the entropy and the dashed ones to the second law of thermodynamics.

$$P(\mu_0 n_0 > l_{inf}) = \int_{-\infty}^{\mu_0 n_0} P(l_{inf}) dl_{inf}, \qquad (30)$$

where $P(l_{sup})$ and $P(l_{inf})$ denote the marginal probability distributions of the upper and lower thermodynamic bounds, respectively. These cumulative probabilities for positive and negative values of α assuming the CPL model are shown in Figures 2 and 3, respectively.

A.
$$\alpha > 0$$

As shown in Figure 2, the probability distribution of the set of cosmological parameters $\{\Omega_m, H_0, w_0, w_a\}$ yields limits where the requirement of positive entropy (solid lines) is more restrictive than the constraint imposed by the second law of thermodynamics (dashed lines). This behavior is also evident in the right panels of Figure 1, where the limits associated with the second law consistently lie at higher values in these distributions. Another important feature is that the most restrictive limits

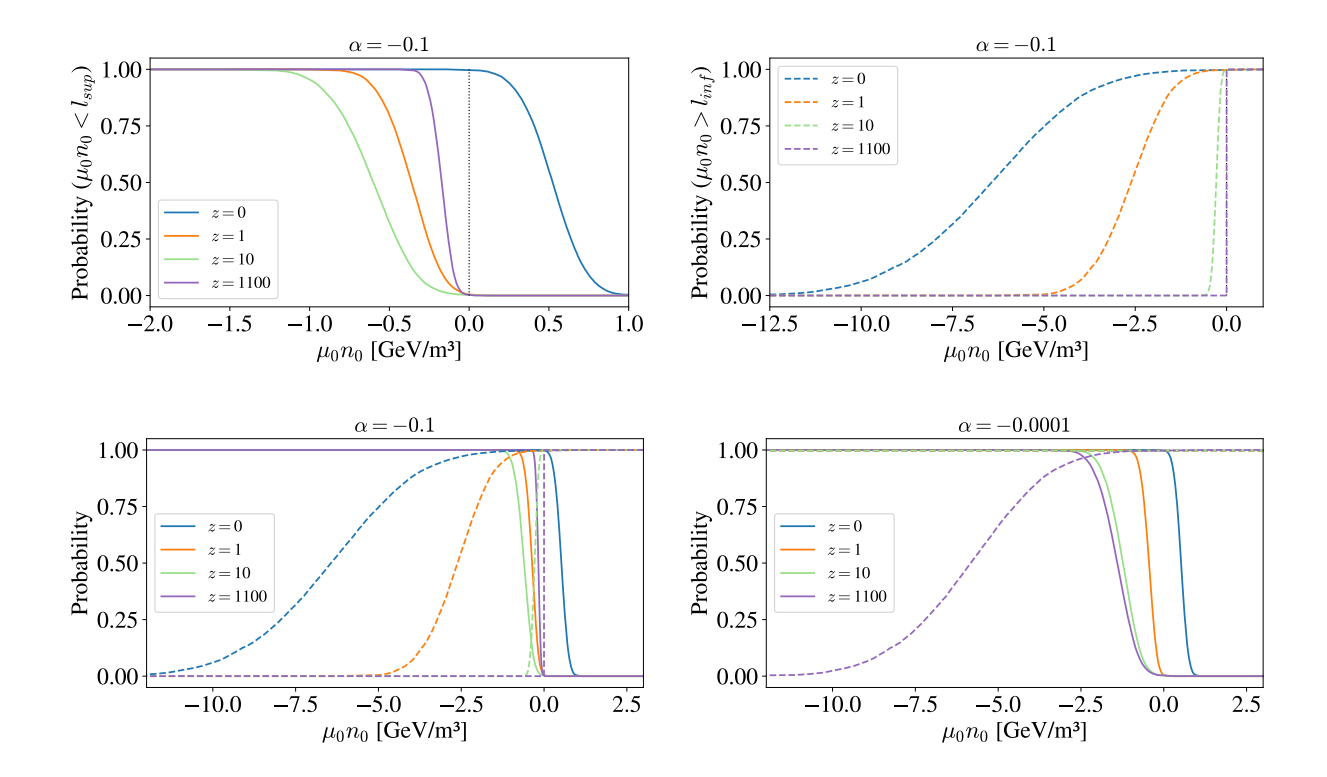


Figure 3. Probability that a given value of $\mu_0 n_0$ satisfies the thermodynamic conditions for negative values of α in the CPL model. The solid lines correspond to the bound of the positivity of the entropy and the dashed ones to the second law of thermodynamics. The dotted line represents the zero limit.

arise from the condition of Eq. (26) and the first condition of Eq. (28) in the highest redshift of the data (z=1100 corresponding to the CMB data). Moreover, an increasing in the value of α further tightens the allowed range of $\mu_0 n_0$.

Since in the cases where $\alpha>0$ both thermodynamic bounds act solely as upper limits, they effectively do not constrain the $\mu_0 n_0$ product of dark energy. Instead, they impose bounds on their possible values. Knowing that the number density is always positive, from Figure 2 it follows directly that the present time value of the fluid chemical potential must be negative, $\mu_0<0$. Since μ/T is assumed to be a constant quantity and bearing in mind that T_0/T is also always positive, $\mu_0<0$ implies $\mu<0$, suggesting a preference for the phantom regime when $\alpha>0$.

B.
$$\alpha < 0$$

Scenarios with negative values of α are particularly interesting due to the existence of both upper and lower thermodynamic bounds. In these cases, the second law of thermodynamics implies the second condition in Eq. (28), thereby constraining the

possible values of the $\mu_0 n_0$ product both from below and above. Figure 3 shows the cumulative probability of a given value of $\mu_0 n_0$ to satisfy the thermodynamic constraints. In the first row of panels, the limits for $\alpha=-0.1$ are displayed independently. When these two conditions are combined (lower-left panel), it becomes evident that no value of $\mu_0 n_0$ satisfy them simultaneously. It is worth mentioning that all limits must be satisfied throughout the entire redshift range of the data; therefore, the most restrictive bounds are adopted, that is, the highest value of the lower limits and the lowest value of the upper limits.

The scenario changes as the parameter α approaches zero from the left. In the low-right panel of Figure 3, a compatibility region appears for $\alpha=-0.0001$, where the effective bounds are determined by the restriction at z=1100. We analyze the behavior of the second law of thermodynamics and the positivity of entropy limits for various negative values of α and find a minimum value of approximately $\alpha=-0.0002$ that allows compatibility between the two thermodynamic bounds. This result establishes a lower limit on α and consequently constrains the possible particle destruction rate in dark energy. For the cases where the values of α allow compatibility

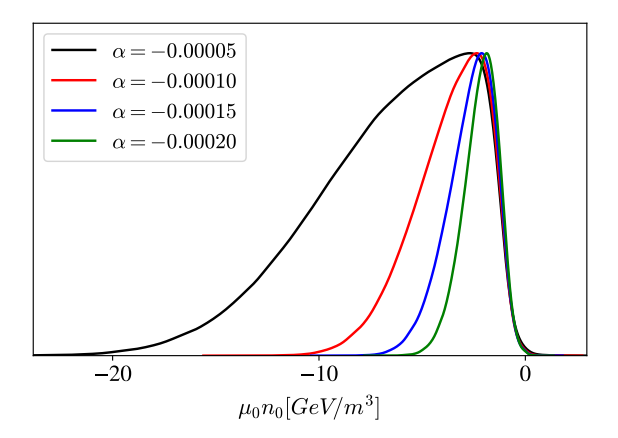


Figure 4. Probability distributions of $\mu_0 n_0$ product for negative values of α .

between both thermodynamic bounds, the product of the chemical potential and the number density can be treated as a random variable, and its probability distribution can be computed as follows.

From the definition of the conditional probability of $\mu_0 n_0$ given the lower and upper limits, $P(\mu_0 n_0|l_{\inf}^{\text{SL}}, l_{\sup}^{\text{PE}})$, which relates the joint probability $P(\mu_0 n_0, l_{\inf}^{\text{SL}}, l_{\sup}^{\text{PE}})$ to the posterior probability of the thermodynamic limits $P(l_{\inf}^{\text{SL}}, l_{\sup}^{\text{PE}})$, we have

$$P(\mu_0 n_0, l_{\inf}, l_{\sup}) = P(\mu_0 n_0 | l_{\inf}, l_{\sup}) P(l_{\inf}, l_{\sup}).$$
(31)

The probability distribution of $\mu_0 n_0$, $P(\mu_0 n_0)$, can then be obtained marginalizing over l_{inf} and l_{sup} ,

$$P(\mu_0 n_0) = \int P(\mu_0 n_0, l_{\text{inf}}, l_{\text{sup}}) \, dl_{\text{inf}} \, dl_{\text{sup}}$$

$$= \int P(\mu_0 n_0 | l_{\text{inf}}, l_{\text{sup}}) \, P(l_{\text{inf}}, l_{\text{sup}}) \, dl_{\text{inf}} \, dl_{\text{sup}}.$$
(32)

For this purpose, it is necessary to define the conditional probability $P(\mu_0 n_0|l_{\inf}^{\mathrm{SL}}, l_{\sup}^{\mathrm{PE}})$. Due to the uncertain nature of dark energy, we assume a flat distribution of $\mu_0 n_0$ conditioned on any pair of limits $\{l_{inf} - l_{sup}\}$, considering only those pairs that satisfy $l_{inf} < l_{sup}$. To estimate the marginalized probability distribution $P(\mu_0 n_0)$, we use the chain provided by the MCMC process in the statistical analysis as a sample of the probability distribution $P(l_{\inf}, l_{\sup})$ (as shown in Figure 1). We then perform a Monte Carlo sampling of $\mu_0 n_0$ by drawing from uniform conditional distributions $P(\mu_0 n_0|l_{\inf}^{\mathrm{SL}}, l_{\sup}^{\mathrm{PE}})$ for each pair of thermodynamic limits $\{l_{inf} - l_{\sup}\}$. The resulting marginalized probability distributions of $\mu_0 n_0$ for various negative values of α , including

its lowest allowed value, are presented in Figure 4. A summary of these distributions, along with their median values and 1σ confidence levels, is provided in Table III.

α	$\mu_0 n_0$
	$[{\rm GeV/m^3}]$
-0.00005	$-6.6^{+5.2}_{-2.0}$
-0.00010	$-3.7^{+2.3}_{-1.1}$
-0.00015	$-2.7^{+1.4}_{-0.8}$
-0.00020	$-2.2^{+1.0}_{-0.7}$

Table III. Constraints on the $\mu_0 n_0$ product considering Pantheon+, DESI DR2, and Planck PR4 data for different values of the parameter α .

It follows that $\mu_0 n_0 (\alpha = -0.0002) = -2.2^{+1.0}_{-0.7} \ GeV/m^3$ is the value of this product for the limiting case of compatibility of the thermodynamic constraints. This quantity becomes more negative as α approaches zero from the left. Therefore, based on arguments similar to those presented in the previous case, the conclusion that the chemical potential must be negative is immediate, indicating a preference for a phantom dark energy when particles are being destroyed in the fluid.

V. CONCLUSIONS

The chemical potential plays a unique role in dark energy thermodynamics. Whether the component is in equilibrium or not, $\mu < 0$ indicates that the fluid is in the phantom regime; $\mu = 0$ recovers the cosmological constant; $\mu > 0$ returns neither of the two cases [10, 11]. By imposing observational constraints on the product of the chemical potential and the number density based on thermodynamic constraints derived from the positivity of entropy and the second law of thermodynamics, the research developed in this work showed that, regardless of the sign of α and considering that n_0 must always be positive, the present time value of the chemical potential of dark energy must be negative, $\mu_0 < 0$. Given that μ/T is considered constant and that T > 0, this leads to the conclusion that the chemical potential must be negative not only in the present, but throughout cosmic history. Therefore, whether particles are being created or destroyed in the component and independently of the cosmic era, we observe $\mu < 0$. This is a strong conclusion, and one that we intend to explore further in a future paper. For now, the results of this current work show a favoring of dark energy models behaving as a phantom fluid, a result compatible with the dark energy behavior at high-zfound by the DESI collaboration [1, 2].

There is, apparently, as seen, no preference regarding the presence of a source or sink of particles in the fluid: in both cases, the chemical potential of dark energy is negative. However, from a theoretical point of view, it is possible to lean towards processes in which particles are destroyed — as we have already argued in [24]. For example, only for $\alpha < 0$ can we impose both an upper and a lower limit on the $\mu_0 n_0$ product, so that, in this scenario, it is possible to establish a range of values for this product. Still within the context of particle destruction, there is a strong indication that the absolute values of α must be very small due to the compatibility of the thermodynamic constraints, according to what is seen in [42, 43]. From this, we establish $\alpha = -0.0002$ as an approximate limit value from which the thermodynamic constraints are compatible and $\mu_0 n_0 (\alpha = -0.0002) = -2.2^{+1.0}_{-0.7} \text{ GeV/m}^3$ as the corresponding value for the product of dark energy chemical potential and number density.

ACKNOWLEDGMENTS

We dedicate this work to the memory of Professor Raimundo Silva, whose contributions to the field of dark energy thermodynamics deeply influenced this study and many others in the field. His scientific vision, intellectual rigor, and generosity as a mentor continue to inspire our research and the wider community. JG acknowledges support from the Foundation for Research and Technological Innovation Support of the State of Sergipe (FAPITEC/SE) under grant number 794017/2013.

Appendix A: BA parameterization results

The difference between the BA and CPL parameterizations leads to significant differences in the corresponding thermodynamic limits. As shown in Figure 5, the correlations between the limits exhibit an opposite behavior at z=1100 in contrast to the CPL results presented in Figure 1. In Figure 6, we present the cumulative probability that a given value of $\mu_0 n_0$ satisfies the thermodynamic bounds. Unlike the CPL parameterization, in the BA model no value of α allows simultaneous compatibility between the positivity of entropy and the second law of thermodynamics. This incompatibility prevents the calculation of the probability distribution of $\mu_0 n_0$.

- A. G. Adame *et al.*, J. Cosmol. Astropart. Phys. 2025, 071 (2025).
- [2] M. Abdul-Karim *et al.*, (2025), 10.48550/arXiv.2503.14738, arXiv:2503.14738 [astro-ph.CO].
- [3] D. Scolnic et al., Astrophys. J. 938, 113 (2022).
- [4] D. Brout et al., Astrophys. J. 938, 110 (2022).
- [5] D. Rubin et al., Astrophys. J. 986, 231 (2025).
- [6] T. M. C. Abbott *et al.*, Astrophys. J. **973**, L14
- [7] N. Aghanim *et al.*, Astron. Astrophys. **641**, A6 (2020).
- [8] N. Aghanim *et al.*, Astron. Astrophys. **641**, A1 (2020).
- [9] J. A. S. Lima and J. S. Alcaniz, Phys. Lett. B 600, 191 (2004).
- [10] J. A. S. Lima and S. H. Pereira, Phys. Rev. D 78, 083504 (2008).
- [11] S. H. Pereira and J. A. S. Lima, Phys. Lett. B 669, 266 (2008).
- [12] R. Silva, R. S. Gonçalves, J. S. Alcaniz, and H. H. B. Silva, Astron. Astrophys. 537, A11 (2012).
- [13] H. H. B. Silva, R. Silva, R. S. Gonçalves, Z-H. Zhu, and J. S. Alcaniz, Phys. Rev. D 88, 127302 (2013).

- [14] J. E. Gonzalez, H. H. B. Silva, R. Silva, and J. S. Alcaniz, Eur. Phys. J. C 78, 730 (2018).
- [15] B. Ratra and P. J. Peebles, Phys. Rev. D 37, 3406 (1988).
- [16] R. R. Caldwell, R. Dave, and P. J. Steinhardt, Phys. Rev. Lett. 80, 1582 (1998).
- [17] I. Zlatev, L. Wang, and P. J. Steinhardt, Phys. Rev. Lett. 82, 896 (1999).
- [18] P. J. E. Peebles and B. Ratra, Rev. Mod. Phys. 75, 559 (2003).
- [19] M. O. Calvão, J. A. S. Lima, and I. Waga, Phys. Lett. A 162, 223 (1992).
- [20] J. A. S. Lima and A. S. M. Germano, Phys. Lett. A 170, 373 (1992).
- [21] W. Zimdahl and D. Pavón, Phys. Lett. A 176, 57 (1993).
- [22] W. Zimdahl, Phys. Rev. D 53, 5483 (1996).
- [23] J. A. S. Lima, A. S. M. Germano, and L. R. W. Abramo, Phys. Rev. D 53, 4287 (1996).
- [24] J. M. Costa Netto and H. H. B. Silva, Chin. J. Phys. 94, 684 (2025).
- [25] M. Chevallier and D. Polarski, Int. J. Mod. Phys. D 10, 213 (2001).
- [26] E. V. Linder, Phys. Rev. Lett. 90, 091301 (2003).

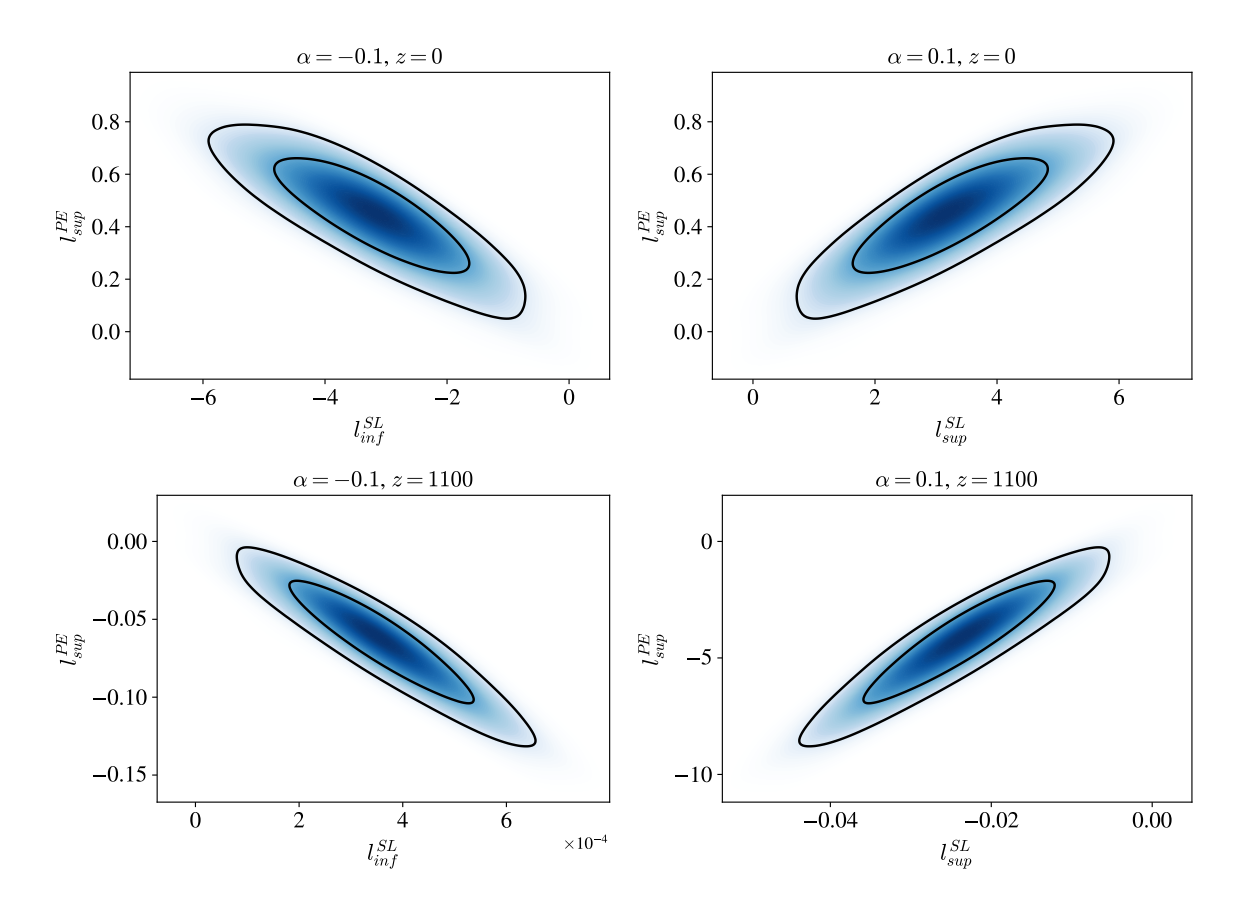


Figure 5. 1σ and 2σ confidence levels of the thermodynamic limits for two values of the parameter α and two redshifts in the BA model.

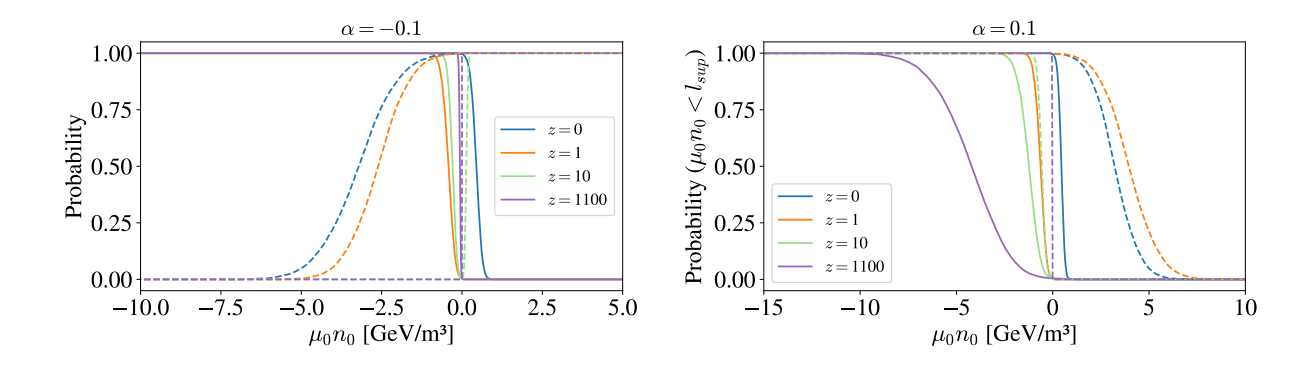


Figure 6. Probability that a given value of $\mu_0 n_0$ satisfies the thermodynamic conditions for two values of α in the BA model. The solid lines correspond to the bound of the positivity of the entropy and the dashed ones to the second law of thermodynamics.

- [27] E. M. Barboza Jr. and J. S. Alcaniz, Phys. Lett. B 666, 415 (2008).
- [28] S. Weinberg, Gravitation and cosmology: principles and applications of the general theory of relativity, 1st ed. (John Wiley and Sons, New York, 1972).
- [29] S. Weinberg, Cosmology, 1st ed. (OUP Oxford, New York, 2008).
- [30] R. Silva, J. A. S. Lima, and M. O. Calvão, Gen. Relativ. Gravit. 34, 865 (2002).
- [31] C. Eckart, Phys. Rev. **58**, 919 (1940).
- [32] L. D. Landau and E. M. Lifshitz, Fluid mechanics: Volume 6 (Pergamon Press, Oxford, 1987).
- [33] E. Gunzig, J. Geheniau, and I. Prigogine, Nature 330, 621 (1987).

- [34] I. Prigogine, J. Geheniau, E. Gunzig, and P. Nardone, Proc. Natl. Acad. Sci. USA 85, 7428 (1988).
- [35] I. Prigogine, Int. J. Theor. Phys. 28, 927 (1989).
- [36] G. Efstathiou and S. Gratton, (2019), 10.21105/astro.1910.00483, arXiv:1910.00483 [astro-ph.CO].
- [37] E. Rosenberg, S. Gratton, and G. Efstathiou, Mon. Not. Roy. Astron. Soc. 517, 4620 (2022).
- [38] J. Carron, M. Mirmelstein, and A. Lewis, J. Cosmol. Astropart. Phys. 2022, 039 (2022).
- [39] J. Torrado and A. Lewis, J. Cosmol. Astropart. Phys. 2021, 057 (2021).
- [40] D. Blas, J. Lesgourgues, and T. Tram, J. Cosmol. Astropart. Phys. 2011, 034 (2011).
- [41] A. Lewis, J. Cosmol. Astropart. Phys. 2025, 025 (2025).
- [42] J. A. S. Lima and J. S. Alcaniz, (1999), 10.48550/arXiv.astro-ph/9902337, arXiv:astro-ph/9902337 [astro-ph.CO].
- [43] J. A. S. Lima and J. S. Alcaniz, (1999), 10.48550/arXiv.astro-ph/9906410, arXiv:astro-ph/9906410 [astro-ph.CO].